A COMBINED MULTI-INSTRUMENTAL APPROACH FOR THE PHYSICO-CHEMICAL CHARACTERIZATION OF STREAM SEDIMENTS, AS AN AID TO ENVIRONMENTAL MONITORING AND POLLUTION ASSESSMENT

Halka Bilinski[1], Stanislav Frančišković-Bilinski[1]*, Marijan Nečemer[2], Darko Hanžel[2], Gábor Szalontai[3] and Kristóf Kovács[3]

[a] Institute "Ruđer Bošković", Division for Marine and Environmental Research, POB 180, HR-10002 Zagreb, Croatia
[b] Institute "Jožef Stefan", Jamova 39, SI-1001 Ljubljana, Slovenia.
[c] University of Pannonia, Department of Silicate and Materials Engineering, Pf. 158, H-8200 Veszprém, Hungary.

ABSTRACT

In the present study we aimed to show on selected sediments from Kupa drainage basin, the advantages of using combined multi-instrumental approach in physico-chemical assessment of sediment quality, with respect to inorganic pollutants. Mössbauer spectroscopy and solid-state magic angel spin nuclear magnetic resonance (^{27}Al and ^{29}Si MAS NMR) methods are recommended in addition to commonly applied techniques: X-ray diffraction (XRD), inductively coupled plasma mass spectroscopy (ICP-MS), X-ray fluorescence(XRF) and grain size analysis, to characterize in details stream sediments. It is suggested that the application of physico-chemical methods, together with a detailed characterization of Fe and Al minerals, is useful in geochemical approach, which is complementary to biological and toxicological tests in TRIAD approach.

From the difference in concentrations of pollutants determined by non destructive XRF and destructive ICP-MS (in aqua regia extract), it is possible to distinguish firmly bound elements: Cr (46-95%), As (84-97%), Pb (29-92%) from loosely bound element Mn (0-8%), which were in some cases above the level causing significant toxicity. The difference is given in percentage as relative scale.

XRD method is useful to determine mineralogical composition of sediment samples. Mössbauer spectroscopy and solid state NMR methods can be used for poorly crystalline and amorphous phases. Quantitative information about the relative population of the iron species together with specific properties of the individual iron sites as oxidation states, and possible iron minerals were obtained by Mössbauer spectroscopy. In the studied samples, the presence and the ratio of tetrahedral and octahedral Al were determined by solid state ^{27}Al MAS NMR. From chemical shifts in comparison with reference spectra of minerals some aluminosilicates (muscovite and kaolinite) were confirmed by solid state ^{29}Si and ^{27}Al MAS NMR methods.

It is recommended that whenever possible it is better to use the two methods (Mössbauer spectroscopy and NMR) in sediment analysis. These methods can be used to follow changes in Fe^{3+}/Fe^{2+} ratio and changes in Al coordination, which are significant in evaluation of precipitation and dissolution processes, which effect pollutant distribution.

Multi-methodical approach on sediments is recommended in the initial phase aimed at identifying minerals which can be useful sinks for pollutants that may pose risks for ecosystems.

KEYWORDS: multi-instrumental approach, stream sediments, physico-chemical characterization, pollution assessment, environmental monitoring.

INTRODUCTION

Stream sediments are formed from the weathering and transport of rocks and erosion of soils. Besides mineral components, organic matter from soils and organic matter formed in the river can be of great importance for their association with pollutants. A geochemical survey usually involves the collection and analysis of numerous samples, with the aim to reveal geochemical signatures and to detect pollution hazards [1, 2]. Although the role of environmental mineralogy was emphasized in the literature [3, 4] it is not widely applied in sediment monitoring. As reported by Förstner and Heise [5], sediments either function as sinks for pollutants or represent a secondary source of pollution, when contaminated particles are mobilized and contaminants released in the water phase. These authors emphasized that an assessment of sediment quality is still prone to several uncertainties and insufficient information. An overview of the sediment quality guidelines (SQGs) in Europe has been given [6]. In the chemical monitoring activ-

ity under the WFD sediments are clearly mentioned with respect to monitoring of priority substances [7]. There is still no decision about which sediment-monitoring approaches will be used in the course of the WFD implementation process, although a Triad approach is used in some of EU countries [8]. In the Triad approach [9], physico-chemical, biological and ecotoxicological assessment methodologies are used. An identical weight is assigned to each of the three assessments. Such complex Triad sediment monitoring program is up to now used in the Netherlands and Belgium, while in some of other highly industrialized countries it is in progress. Triad approach is not yet used in less polluted environments. An example is Kupa transboundary drainage basin (Croatia, Slovenia, Bosnia and Herzegovina), which is in focus of our recent studies [10-15]. Major trends in trace elements and baseline values have been determined [13]. Toxic substances, including organic pollutants were highlighted [10] using the existing criteria of SMSP and Falconbridge NC, SAS [16]. Quality of sediments of the Kupa drainage basin was not yet assessed with respect to ecosystem and human health. Only in preliminary work on barium contamination in Lokve, Croatia, risks on human health were discussed [17]. As a combination of geochemical, mineralogical and biological approaches is the optimal approach nowadays, first attempts are performed on Sava River, within SARIB project, part of FP6. Sava River is a recipient of Kupa River. Fish (*Leuciscus, cephalus, L.*) was studied as bioindicator of Sava River water quality [18]. There was also attempt to determine the chronic toxicity of river water, organic sediment extracts and sediment pore water from the Sava River to the algae *Pseudokirchneriella subcapitata* [19]. Only a crude risk assessment identified that some of the locations in Sava River may represent a risk to algae. The authors have concluded that multiple bioassays and exposure phases are required to conduct a thorough risk assessment of Sava River sediments and surface water.

The aim of the present work

The aim of the present study was to continue our preliminary work [20] and use combined multi-instrumental approach for detailed sediment characterization in the first part of TRIAD approach. It is hypothesized that in addition to chemical characterization, environmental mineralogy can provide valuable information on binding phases and as such on pollution sinks or sources in any river system. Biological and ecotoxicological tests could be independently performed when necessary for thorough risk assessment. The results could help to establish monitoring network and water management in accord with the European Framework Directive [21].

MATERIALS AND METHODS

Sampling of the sediments

In order to illustrate the application of complementary multi-instrumental approach, four selected stream-sediment samples were chosen from the large dataset of the transboundary Kupa River drainage basin of Frančišković-Bilinski [11, 13], where location map is presented. From the chosen samples, three show various anomalies, determined from the geochemical dataset by the box plot method [22]: sample 23 (Nb, V, Mn, Zr); sample 24 (Sc, V, Zr, Na, Fe, Cu, Ga, Y); sample 14R (Mn, Pb, Zn). Comparison of anomalous concentrations of elements with lithological back-ground values [13] shows that they are 5 – 6 times higher for Mn, 3 times higher for Pb and Cu, 2.5 times higher for Zn and 2.2 times higher for Fe. Sample 41 belongs to the cluster of samples without any anomaly. The samples were air-dried in the shade for several days, after which the material was dry sieved using standard sieves (Fritsch, Germany). The fraction of silt + clay (<63 μm) was subsequently analyzed using a complementary multi-instrumental approach.

Measurements and analysis

The mineralogical composition was determined using a Philips X-Pert MPD x-ray diffractometer. The crystalline phases obtained using a computer program (X'Pert High score 2002, Philips) were selected by comparing d-values from the JCPDF cards listed in the Powder diffraction file [23]. Semi-quantitative mineralogical compositions were determined by comparing the strongest intensities of detected minerals, as described in Boldrin et al. [24].

The elements were determined in aqua regia extract at the ACTLABS commercial laboratory, Ontario, Canada in the fraction <63 μm, using ICP-MS (inductively coupled plasma mass spectroscopy) and the program "Ultratrace 2". The solution was diluted and analyzed using a Perkin Elmer SCIEX ELAN 6100 ICP-MS instrument. For the analyses the following reference materials were used: USGS GXR-1, GXR-2, GXR-4 and GXR-6. Units given in ppm represent mg/kg. Reported detection limits range at the $ngkg^{-1}$ level, or lower for most elements. Although this digestion is not total, its use is justified because the international standard methods for determining action limits are based on aqua regia leach [25].

The experimental set up for XRF analysis, calibration and quantitative analysis were described by Kump et al. [26]. The x-ray fluorescence analysis system consisted of an x-ray spectrometer, a set of annular radioisotopic excitation sources, and spectrum analysis and quantification software. An x-ray spectrometer with a Si (Li) detector, an integrated signal processor (M1510, Canberra), and a PC-based MCA card (S-100, Canberra) was utilized. A spectrometer resolution of about 175 eV at 5.9 keV was achieved. For the excitation, the annular radioisotopic sources, Cd-109 (8 mCi), Fe-55 (10 mCi) and Am-241 (25 mCi) (Isotopes Products Laboratories, U.S.A.) were utilized. The spectrum-acquisition time was 10,000 s (Cd-109), and 5,000 s (Am-241 and Fe-55). The measurements of samples using Cd-109 and Am-241 were performed in air. The samples analyzed with the radioisotopic source Fe-55 were in vacuum. The pulverized and homogenized samples were prepared

by pressing them into a pellet using a pellet die and a hydraulic press. The x-ray spectra were analyzed by the AXIL spectrum analysis program, according to the method of Van Espen and Janssens [27]. The error evaluated from the AXIL program included the statistical errors of the measured x-ray intensities, as well as the errors in the mathematical procedure utilized when fitting the experimental spectral data. The overall uncertainty was, in most cases, less than 1%. The quantification and estimation of the combined standard uncertainty (u) was done utilizing the QAES (quantitative analysis of environmental samples) software developed by Kump et al. [26]. The sensitivities were determined from measurements on standard NIST-SRM-2704 River Sediment. The average values of the concentrations for the major and minor constituents were, in most cases, within 5% of the reference data. However, the accuracy of the trace-element determinations was worse (10% and more). The details about NIST-SRM-2704 are given in Certificate of analysis of National Bureau of Standards [28].

The particle size distribution was determined in the <63 μm fraction using an "Analysette 22" laser particle sizer (Fritsch Gmbh) and a Mini Cell for particle sizes <100 μm. A helium-neon laser with a wavelength of 0.6328 μm was used. According to the operating principle, when a spherical particle is illuminated, a "Frauenhofer diffraction pattern" is produced. The diameter of the particle can be calculated. The surface area automatically recorded represents geometric surface area.

Poorly crystalline iron minerals were studied using Mössbauer spectroscopy at 300 and 70 K. For all the experiments a ^{57}Co source was used with an activity of ~10 mCi in a Rh matrix. The velocity scale was calibrated with metallic Fe, which was also used as a reference for the isomer shift parameters. The speciations were computer fitted by assuming Lorentzian or Voigt shapes for the resonance lines. The best least-squares fit parameters were used for the characterization of the Fe-containing phases. For each sample Fit Summary contains number of data points, number of doublets in model, number of parameters in model, number of refined parameters and reduced χ^2. Uncertainties are calculated using the covariance matrix.

The solid-state NMR experiments on sediment samples were performed on a Varian UNITY 300 NMR spectrometer equipped with a room-temperature double-bearing Doty XC5 probe. At 7.04 Tesla the ^{29}Si resonance frequency, $\omega_o/2\pi$ was -59.585 MHz. The ^{27}Al resonance frequency, $\omega_o/2\pi$ was -78.172 MHz. The spectra were recorded with high-power (~100-120 W) proton decoupling. The sample spinning speeds were typically varied between 4000 and 8500 Hz. Samples with masses of 90-120 mg were used in 5-mm o.d. zirconium or Si_3N_4 rotors. The number of scans was about 800-1800 for the ^{29}Si spectra (pw_{90}^o 4.6 μs) and about 512 for the ^{27}Al spectra (pw_{90}^o 2.6 μs, only the central (+/- ½) transitions were exited). The ^{29}Si and ^{27}Al MAS spectra were recorded with recycling delays of 20-120 and 2-4 s, respectively. The ^{29}Si 90° pulse width was about 3.6 μs. In the case of silicon, for referencing purposes, kaolinite was used (δ = - 92 ppm relative to the TMS) with the substitution method. The ^{27}Al chemical shifts were given relative to the external $Al(H_2O)_6^{3+}$.

The MQMAS experiments and the 9.39 T ^{27}Al spectra were recorded on a Bruker AV400SB Instrument (pulse sequence mp3qzfq.av) operating at 400 MHz (^{27}Al $\omega_o/2\pi$ - 104.261 MHz). Zirconia rotors of 4 mm were used in these cases and the rotation speed varied between 10,000 and 14,000 Hz.

RESULTS

X-ray diffraction (XRD)

A semi-quantitative mineralogical analysis was performed as described in Boldrin et al. [24]. The most predominant mineral (>30%) in all the samples is quartz (JCPDF 46-1045). This is followed (10-30%) by the mica group from the phyllosilicate class (muscovite) in samples 23 (JCPDF 07-0032) and 14R (JCPDF 01-1098). The feldspar, plagioclase group from the tectosilicate class (albite, JCPDF 09-0466) is present in sample 24. Calcite (JCPDF 05-0586) is present in samples 23, 24 and 41 in amounts of 5 to 10%. Of the other minerals, baileychlore (JCPDF 42-1335), from the chlorite group, phyllosilicate class was found in sample 24. Anorthite (JCPDF 20-0528) from the feldspar plagioclase group was found in sample 14R. Various trace minerals (<5%), suggested from XRD patterns, could not be identified with certainty. These were: dolomite, clinochlore, anorthoclase and biotite ferrian in sample 23; muscovite, kaolinite, microcline and dolomite ferroan in sample 24; anorthite, illite and dolomite in sample 41; clinochlore ferroan in sample 14R.

Elemental analysis

To illustrate the advantages or disadvantages of two techniques used for elemental analysis, the data are presented. The results obtained by the ICP-MS method are presented in Table 1, and those from the XRF method are in Table 2. The two multi-elemental techniques are often used in sedimentary research as complementary methods. Salomon et al. [29] have described the practical aspects of routine trace-element analysis with the ICP-MS method. The details of the XRF method can be found in literature [26, 27]. They provide full details on the precision and accuracy of the analysis, which will not be repeated in the present paper. Results of elemental analyses obtained by the two methods will be discussed in details in the Discussion part.

Grain size analysis

The particle size distribution was measured in fraction <63 μm to obtain the amount of clay-size material. According to Wentworth [30] the silt-clay boundary is <4 μm. Corresponding geometric surface area was automatically recorded. Sample 23 contains 12.64% of clay-size material,

with a geometric surface area of 0.9290 m^2/g. Sample 24 contains 8.31% of clay-size material, with a geometric surface area of 0.7015 m^2/g. Sample 41 contains 7.41% of clay-size material, with a geometric surface area of 0.6080 m^2/g. Sample 14R contains 8.00% of clay-size material, with a geometric surface area of 0.7121 m^2/g. The results are presented in Figure 1 (a-d).

Mössbauer spectroscopy

Poorly crystalline and amorphous Fe compounds can be characterized using Mössbauer spectroscopy. The Mössbauer spectra of the studied sediment samples (f <63 μm) were first recorded at 300 K. The deconvolution shows that they exhibit four paramagnetic doublets in samples 23, 41 and 14R, and five paramagnetic doublets in sample 24. The hyperfine parameters of the Mössbauer spectra are presented in Table 3; they indicate the presence of Fe^{2+} and Fe^{3+} environments in different proportions for each sample.

TABLE 1 - Concentrations of 51 element in selected stream sediments determined by ICP-MS method.

Element / sample	23	24	41	14R
Ca (%)	2.73	4.17	3.62	1.01
Al (%)	2.00	1.94	0.66	1.65
Fe (%)	2.80	3.87	1.42	3.01
Mg (%)	0.99	1.73	0.70	0.58
K (%)	0.19	0.19	0.04	0.13
S (%)	0.042	0.045	0.080	0.063
P (%)	0.051	0.062	0.034	0.076
Na (%)	0.012	0.046	0.007	0.014
Li (ppm)	20.8	23.6	8.0	23.7
Be (ppm)	0.8	0.8	0.4	0.8
Sc (ppm)	4.9	9.9	1.8	2.1
V (ppm)	45	125.	14	20
Cr (ppm)	40.5	44.1	19.3	23.3
Mn (ppm)	2260	1470	291	2640
Co (ppm)	16.5	19.3	7.0	13.3
Ni (ppm)	47.6	39.8	20.9	25.3
Cu (ppm)	29.9	50.0	8.9	17.6
Zn (ppm)	77.2	72.5	42.2	133.9
Ga (ppm)	5.61	7.85	2.12	4.38
As (ppm)	5.4	1.0	2.0	9.4
Se (ppm)	0.3	0.7	0.3	0.4
Rb (ppm)	14.6	11.5	5.3	15.9
Sr (ppm)	26.0	37.6	29.6	17.4
Y (ppm)	9.77	14.32	5.59	6.18
Zr (ppm)	3.0	7.6	0.6	1.4
Nb (ppm)	2.1	0.9	0.3	0.6
Mo (ppm)	0.60	0.47	0.32	0.54
Cd (ppm)	0.3	-0.5	0.2	0.4
Sn (ppm)	0.38	-0.25	0.14	0.58
Sb (ppm)	0.22	0.26	0.09	0.27
Cs (ppm)	1.1	1.7	0.5	1.7
Ba (ppm)	111	271	54	158
La (ppm)	17.7	11.4	7.7	15.9
Ce (ppm)	37.3	28.9	15.9	34.7
Pr (ppm)	4.3	3.3	1.9	3.8
Nd (ppm)	16.7	14.3	7.5	14.0
Sm (ppm)	3.4	3.6	1.7	2.9
Eu (ppm)	0.7	0.9	0.3	0.5
Gd (ppm)	3.2	3.7	1.7	2.6
Tb (ppm)	0.4	0.6	0.2	0.3
Dy (ppm)	2.2	3.3	1.2	1.5
Ho (ppm)	0.4	0.6	0.2	0.3
Er (ppm)	1.0	1.5	0.5	0.6
Yb (ppm)	0.9	1.2	0.4	0.6
Au (ppm)	0.009	-0.001	0.005	0.015
Tl (ppm)	0.17	0.12	0.10	0.17
Pb (ppm)	18.6	15.3	9.1	51.5
Bi (ppm)	0.21	0.43	0.07	0.25
Th (ppm)	3.3	2.9	2.3	3.6
U (ppm)	0.6	0.5	0.5	0.8
Hg (ppm)	0.058	0.021	0.067	0.120

TABLE 2 - Concentrations of 23 elements in selected stream sediments determined by XRF method and three sources (Fe, Cd and Am)

Element/ sample	2 3			2 4			4 1			1 4 R		
	source Fe	Source Cd	Source Am	Source Fe	Source Cd	Source Am	Source Fe	Source Cd	Source Am	Source Fe	Source Cd	Source Am
Al (%)	8.58	-	-	9.64	-	-	6.75	-	-	11.1	-	-
Si (%)	27.8	-	-	27.6	-	-	33.9	-	-	29.7	-	-
K (%)	1.91	1.97	-	1.24	1.01	-	1.09	1.01	-	2.23	2.19	-
Ca (%)	3.67	3.65	-	5.39	5.41	-	4.82	5.07	-	1.25	1.31	-
Ti (%)	0.515	0.594	-	0.620	0.875	-	0.384	0.651	-	0.468	0.595	-
V (ppm)	-	206	-	-	281	-	-	217	-	-	220	-
Fe (%)	-	3.22	-	-	4.33	-	-	1.78	-	-	3.64	-
Cr (ppm)	-	75.6	-	-	118	-	-	380	-	-	99.7	-
Mn (ppm)	-	2040	-	-	1330	-	-	279	-	-	2870	-
Ni (ppm)	-	31.4	-	-	52.2	-	-	27.0	-	-	19.1	-
Cu (ppm)	-	17.7	-	-	49.3	-	-	25.3	-	-	31.4	-
Zn (ppm)	-	74.5	-	-	83.2	-	-	60.8	-	-	169	-
Br (ppm)	-	7.50	-	-	2.28	-	-	2.60	-	-	6.61	-
Pb (ppm)	-	100	-	-	87.1	-	-	115	-	-	72.9	-
As (ppm)	-	34.1	-	-	38.8	-	-	33.2	-	-	-	-
Rb (ppm)	-	69.4	-	-	47.1	-	-	44.9	-	-	97.2	-
Sr (ppm)	-	95.3	-	-	109	-	-	79.0	-	-	71.9	-
Y (ppm)	-	24.1	-	-	28.6	-	-	24.3	-	-	21.2	-
Zr (ppm)	-	296	-	-	418	-	-	103	-	-	493	-
Nb (ppm)	-	14.9	-	-	9.06	-	-	13.9	-	-	12.5	-
Ba (ppm)	-	-	334	-	-	437	-	-	227	-	-	558
La (ppm)	-	-	27.8	-	-	19.6	-	-	39.4	-	-	37.7
Ce (ppm)	-	-	58.6	-	-	47.9	-	-	76.4	-	-	80.5

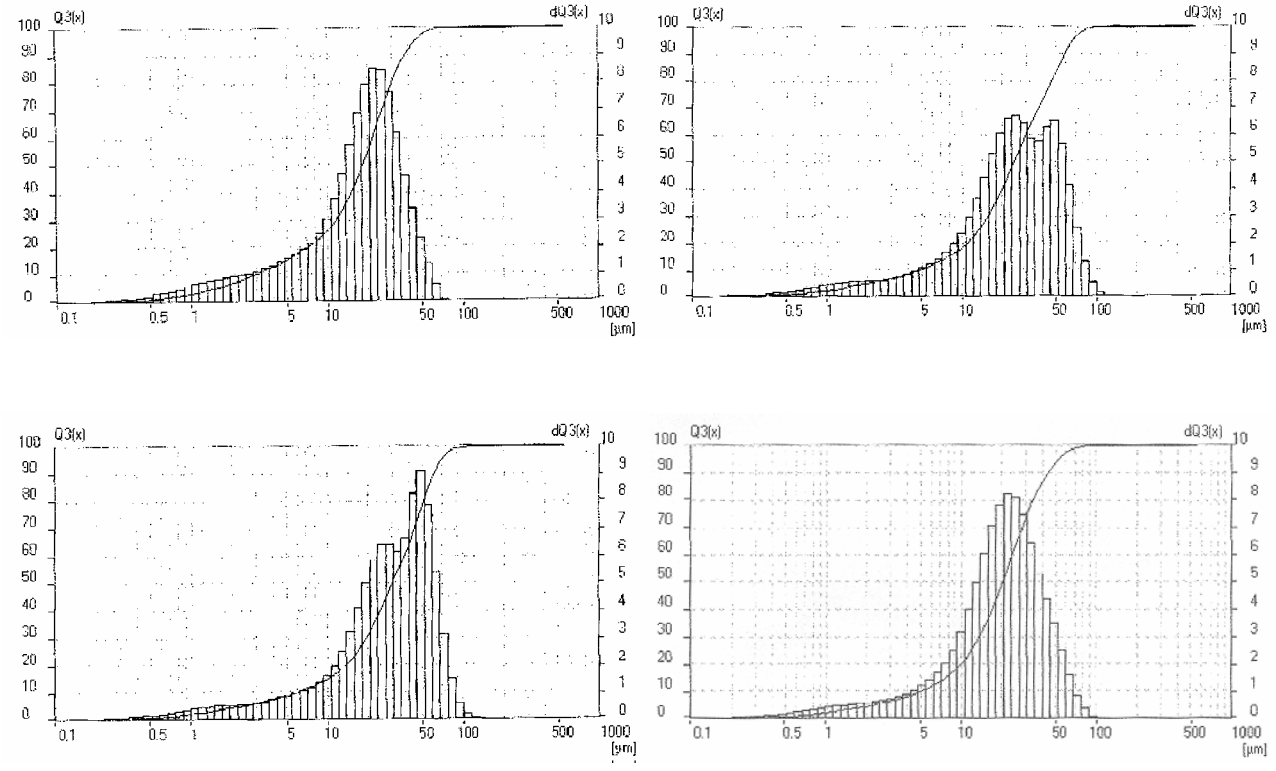

FIGURE 1 - Grain size analysis in <63 µm fraction of sediment samples: a (sample 23), b (sample 24), c (sample 41), d (sample 14R), performed by "Analysette 22" laser particle sizer and Minicell.

TABLE 3 - Hyperfine parameters of the Mössbauer spectra of selected stream sediments (f <63 µm) from Kupa River drainage basin at 300 K

Sample	Sub-spectra	IS mm s^{-1}	QS mm s^{-1}	Site	A %	Fe^{3+} %	Fe^{2+} %	Fe^{2+} oct. %	Fe^{2+} tetr. %	Fe^{3+} / Fe^{2+}
	du 1	0.376 (22)	0.656 (13)	Fe^{3+}	64.5 (29)					
23	du 2	0.95 (95)	0.8(19)	Fe^{2+}	2.6 (13)	64.5	35.5	28.6	6.90	1.82
	du 3	1.109 (32)	2.639 (24)	Fe^{2+}	28.6 (24)					
	du 4	0.607 (28)	0.925 (60)	Fe^{2+}	4.3 (10)					
	du 1	0.393 (13)	0.554 (44)	Fe^{3+}	35.3 (59)					
	du 2	0.41 (11)	0.94 (31)	Fe^{3+}	21.1 (60)	56.4	43.6	38.9	4.7	1.29
24	du 3	1.118 (13)	2.638 (27)	Fe^{2+}	31.7 (18)					
	du 4	0.986 (24)	0.879 (46)	Fe^{2+}	4.7 (9)					
	du 5	1.02 (14)	2.14 (27)	Fe^{2+}	7.2 (16)					
	du 1	0.370 (16)	0.557 (54)	Fe^{3+}	42.8 (10)					
41	du 2	0.903 (49)	1.020 (95)	Fe^{2+}	6.5 (50)	51.1	48.9	42.4	6.5	1.04
	du 3	0.349 (31)	1.032 (68)	Fe^{3+}	8.3 (34)					
	du 4	1.076 (30)	2.576 (60)	Fe^{2+}	42.4(58)					
	du 1	0.3696 (52)	0.478 (37)	Fe^{3+}	25.5 (52)					
14R	du 2	1.1198 (92)	2.649 (18)	Fe^{2+}	23.5 (87)	76.5	23.5	23.5	-	3.26
	du 3	0.360 (11)	0.767 (99)	Fe^{3+}	40.6					
	du 4	0.48 (16)	1.14 (27)	Fe^{3+}	10.4 (92)					

[a] IS/mms^{-1}, isomer shift relative to metallic iron; QS/mms^{-1}, electric quadrupole splitting; A/%, relative resonance area in percent of total iron

TABLE 4 - Hyperfine parameters of the Mössbauer spectra of selected stream sediments (f<63 µm) from Kupa River drainage basin at 70K

Sample	Subspectra	IS mms^{-1}	QS mms^{-1}	H_{eff} (kOe)	Site	A%
23	du1	0.465(11)	0.770(16)	-	Fe^{3+}	46.1(10)
	du2	1.270(15)	2.886(26)	-	Fe^{2+}	22.8(14)
	se1	0.493(26)	-0.098(21)	529.9(14)	Fe^{3+}	13.0(15)
	se2	0.502(47)	-0.220(47)	468.2(39)	Fe^{3+}	18.1(23)
24	du1	1.236(66)	2.863(13)	-	Fe^{2+}	35.4(13)
	du2	0.477(13)	0.716(22)	-	Fe^{3+}	38.0(17)
	du3	0.858(71)	1.760(12)	-	Fe^{2+}	5.5(19)
	se1	0.500(58)	-0.210(56)	462.6(38)	Fe^{3+}	21.1(26)
41	du1	1.384(12)	2.462(23)	-	Fe^{2+}	36.4(22)
	du2	0.294(12)	0.945(23)	-	Fe^{3+}	41.7(18)
	se1	0.537(52)	-0.135(52)	470.1(35)	Fe^{3+}	21.9(36)
14R	du1	0.464(14)	0.863(88)	-	Fe^{3+}	34.0(87)
	du2	1.225(15)	2.966(30)	-	Fe^{2+}	21.2(16)
	du3	0.446(29)	0.352(93)	-	Fe^{3+}	6.9(72)
	du4	0.862(41)	1.811(80)	-	Fe^{2+}	2.8(14)
	se1	0.446(36)	-0.151(35)	475.5(26)	Fe^{3+}	35.1(34)

In sample 23 there is an indication of the presence of two Fe^{3+} and two Fe^{2+} environments. Phyllosilicates contain Fe^{2+} and Fe^{3+} ions at different crystallographic sites and in different valence states. The values of the hyperfine parameters of the doublet sub-spectra (labeled) du1 and du3 suggest Fe^{3+} and Fe^{2+} in phyllosilicates, where du3 is presumably a single ferrous doublet of chlorites [31]. Similar values were obtained for Pinal Creek samples [32].

Sample 24 appears to contain two Fe^{3+} and three Fe^{2+} environments. Here the doublets (labeled) du3 and du5 are presumably two ferrous doublets of a 2:1 layer mineral of the mica group.

Sample 41 appears to contain two Fe^{3+} and two Fe^{2+} environments. The doublet (labeled) du1 is interpreted as representing Fe^{3+} in the octahedral sites of amorphous Fe oxides. The doublet (labeled) du4 could represent Fe^{2+} in illite.

In sample 14R there appears to be three Fe^{3+} and one Fe^{2+} environment. The doublet (labeled) du2 is interpreted as representing Fe^{2+} in chlorite (clinochlore ferroan).

Mössbauer spectra were also taken at 70 K. We can offer only a tentative explanation. They show, in addition to paramagnetic doublets, one magnetically split sextet pattern in samples 24, 41 and 14R and two sextet patterns in sample 23. The hyperfine parameters of the Mössbauer spectra taken at 70 K are presented in Table 4. The two sextets in sample 23 could be interpreted as non-stoichiometric Fe oxides present in the form of small particles, because the room-temperature spectra of the same sample do not show any magnetic contribution. The relaxation of the direction of magnetization in small particles slows down with decreasing temperature. When the jump times are comparable or longer than the time window of Mössbauer spectroscopy (100ns) the averaging effect of a fluctuating magnetic field is no longer present and magnetically resolved spectra appear. The sextet pattern (labeled se1), with an effective magnetic field of 530 kOe, in sample 23, could be identified as hematite, α-Fe_2O_3, and the sextet pattern (labeled as se2), with an effective magnetic field of 468 kOe, could be identified as goethite, α-FeO(OH). In sample 24, the sextet pattern (labeled as se1) with an effective mag-

netic field of 463 kOe could be identified as goethite, α-FeO(OH). The sextet patterns (labeled as se1) in samples 41 and in 14R, which probably suggest the presence of goethite, could not be explained with certainty.

Solid-state NMR

Solid-state NMR spectroscopy, like Mössbauer spectroscopy, can be used for characterization of amorphous and crystalline compounds. In the present work, using ^{29}Si MAS NMR and ^{27}Al MAS NMR, additional information could be obtained about Al and Si containing minerals, which were suggested by the XRD method.

The proper reference spectra of the minerals were taken and the chemical shifts compared. Results will be described for each sediment sample. As an illustration the spectra will only be presented for selected samples (41 and 14R) in Figure 2 (a, b) and Figure 3 (a, b).

Sample 23: ^{29}Si MAS NMR: from the observed chemical shifts the presence of muscovite Q3(mAl) is likely, what is in support to the result obtained by XRD. There are unresolved signals at about -81, -85 and -89 ppm, but there are additional signals at -93.5, -97.6 and -101.6 ppm, which correspond to the literature values of microcline.

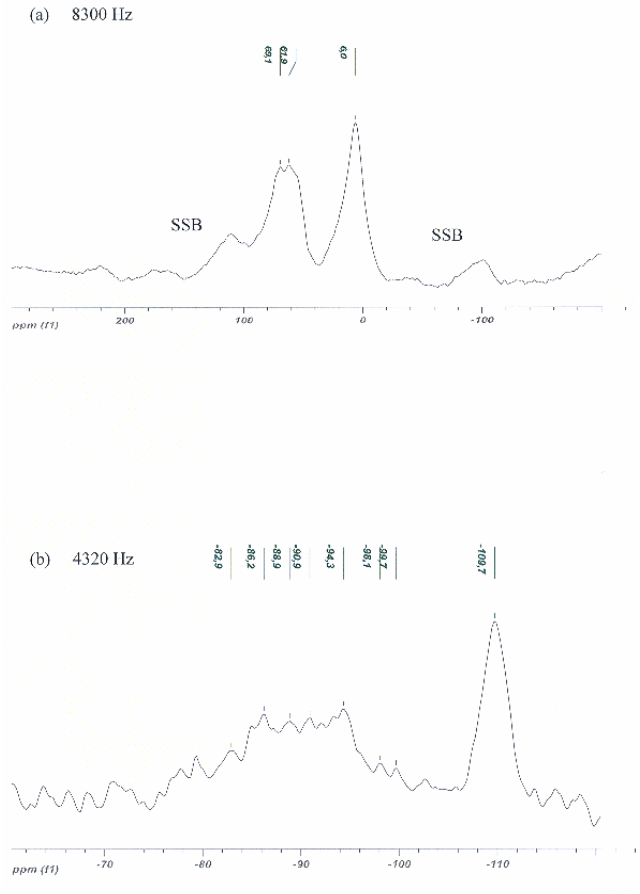

FIGURE 2 - ^{27}Al NMR (a) and ^{29}Si NMR (b) MAS spectra of sample 41 recorded at rotation speeds of 8300 and 4320 Hz, respectively. (SSB = spinning side bands)

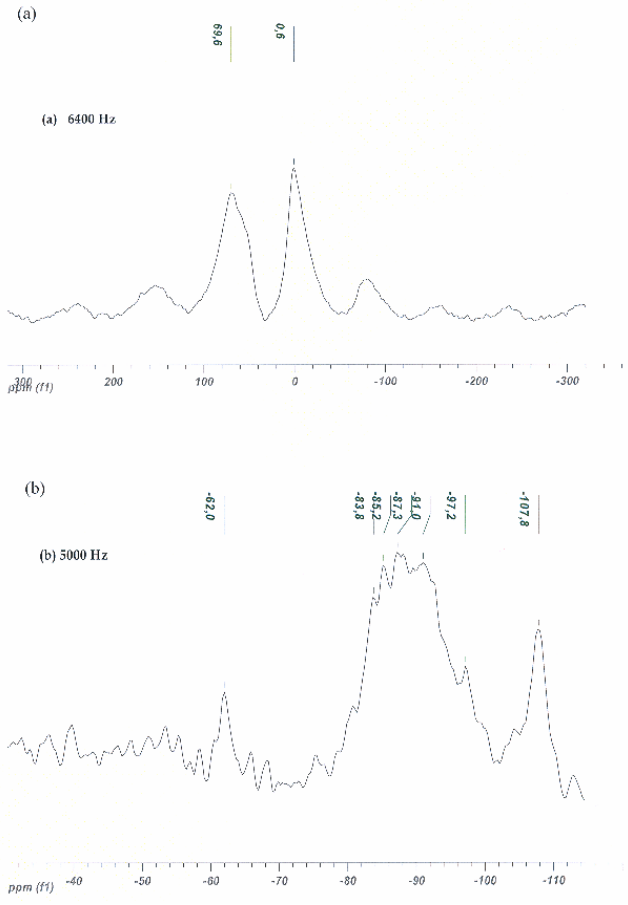

FIGURE 3 - ^{27}Al NMR (a) and ^{29}Si NMR (b) MAS spectra of sample 14R.

However, the low signal-to-noise ratio of the spectrum prevents an unambiguous assignment [33]. The signal at -107 ppm can be assigned to the α-quartz (Q4(0Al)) content of the sample. The weaker signals between -91.5 and -98.5 ppm are evidence for the presence of phyllosilicates (e.g., clinochlore, biotite ferrian), what is also in agreement with XRD result.

The ^{27}Al MAS spectrum also suggests a substantial amount of muscovite and/or other species, which contain both tetrahedrally and octahedrally coordinated Al atoms. The tetrahedrally coordinated Al atoms (most likely in Al_tOAl_o and Al_tOSi environments) are clearly seen at about 71.8 and 61.2 ppm. The reported chemical shifts are uncorrected for the second-order quadrupole effect [34].

The somewhat stronger signal at 7.8 ppm can be assigned to octahedrally coordinated aluminium (most likely Al_oOAl or Al_oOSi). The estimate of the ratio for four-coordinate and six-coordinate Al atoms is about 55:45.

Sample 24: ^{29}Si MAS NMR: this sample produced the weakest spectrum. The relatively narrow signal at –109.4 ppm can be assigned to the quartz. The broad signal between -85 and -100 ppm allows the presence of kaolinite, what is in accord with XRD. The presence of a substantial amount of albite cannot be confirmed, what does not support the finding by XRD.

^{27}Al MAS spectrum: The tetrahedrally coordinated Al atoms are clearly seen at 54.1 ppm. The signal at 0.0 ppm can be assigned to octahedrally coordinated aluminium. The estimate of the ratio for the four-coordinate and six-coordinate Al atoms is about 55:45.

Sample 41: ^{29}Si MAS NMR: the spectrum is similar to that of sample 23. However, the relative ratio of the Q^4(0Al) species (– 109.4 ppm silica gel) is about twice as large.

^{27}Al MAS spectra: the spectrum recorded at 7 T is also similar to that of sample 23, the estimate of the ratio for the four-coordinate and six-coordinate Al atoms is about 1:1. In this case, there are two chemically different tetrahedral sites for the Al atoms or, alternatively, strong second-order quadrupole effects are present since the signal at about 70.0-58.1 ppm is split. To get rid of the latter the MQMAS spectrum [35, 36] of the sample was also recorded at 9.38 T. This clearly proved the presence of two different environments for the tetrahedral Al atoms.

Sample 14R: ^{29}Si MAS NMR: there is a signal at -61.7 ppm, a broad unresolved multiplet between – 80 and - 98 ppm, and another singlet at -108 ppm. The high- and low-frequency resonances can be assigned to the Q^0 and Q^4(0Al) species, respectively. The broad multiplet in between seems to be a mixture of the muscovite (with a disordered Si and Al distribution) and microcline signals. The finding of muscovite supports XRD results.

^{27}Al MAS spectrum: there are two resonances, a smaller one at 69.6 ppm, which can be assigned to the four-coordinate atoms and a larger one at about 0.6 ppm, which can be assigned to the octahedrally coordinated aluminium atoms. The ratio of the four-coordinate and six-coordinate Al atoms is near to 30:70. The ratio of the six-coordinated to four-coordinated Al atoms approximately corresponds to 2, which has been reported for natural muscovite [37].

DISCUSSION

X-ray diffraction (XRD)

Trace minerals (<5%) belong to carbonate class (dolomite, dolomite ferroan), to tectosilicate class (anorthoclase and anorthite) and all others to phyllosilicate class. This phyllosilicate class is significant for any discussion of weathering of the studied region. According to Wang and Valentine [38], weathering of phyllosilicates in an acidic environment yields clay minerals like kaolinite, while in an alkaline environment it yields montmorillonite. It is very possible, referring to [38] that a low-temperature hydrothermal alteration produced the chlorites and micaceous minerals in samples 23, 24 and 14R. In this region, which is a part of Supradinaric belt, sedimentation was under the influence of penetration of mafic and ultramafic lavas and also of younger neutral and acid volcanism, as described in Frančišković-Bilinski [13]. From the fact that kaolinite is present in sample 24 and that montmorillonite was not found, as was observed in different environment of the boreal region [39], it is probable that in the present study area the weathering occurred in an acidic environment. The biotite ferrian in sample 23 can form as a result of the hydrothermal alteration of biotite, according to the weathering study of Wang and Valentine [38]. Presented XRD results provide insights to the bulk mineralogy of sediments, what is important in understanding adsorption affinity to organic matter and to trace elements, as reviewed by Brown and Parks [40]. Thus XRD method, together with the knowledge about the adsorption processes, can be indirectly related to sediment quality evaluation.

Elemental analysis

According to Skoog et al. [41], a particular advantage of XRF is that it is in contrast to most other elemental analysis techniques, non destructive of the sample. It is very suitable for the easy determination of major elements. The concentrations of Si and Al can be determined with the Fe source. The concentrations of K and Ca, determined with the Fe and Cd sources are in relatively good agreement. However, the major elements Mg and Na could not be detected, and the concentrations of Ti, determined with the Fe and Cd sources are in poor agreement (see Table 2).

The ICP-MS method is suitable for determining major elements (Mg and Na included), however Si cannot be measured. It is not, however, suitable for determining the Ti concentration, which is near or below the detection limit. For this reason it was omitted from Table 2. When the results obtained using the two methods are compared, the values for the major elements obtained with XRF are higher than those obtained with ICP-MS. The reason is that the ICP-MS method requires chemical decomposition, and the dissolution in aqua regia was incomplete.

The number of trace elements determined with available XRF equipment was limited to 17; this is small in comparison with 43, determined with the ICP-MS. An additional standard, NIST SRM 2710 (Montana Soil), was used to check the XRF results for minor elements. The details about this standard are given in Certificate of analysis of National Bureau of Standards (2002). For trace and ultra-trace element analyses the ICP-MS is more suitable than the XRF. If one compares differences in percentage as relative scale of pollutants determined by ICP-MS and XRF, one can conclude that 95% of Cr is bound in sediment 41, which has its highest concentration. Therefore extensive biological and toxicological studies for Cr at this location can be avoided. Other pollutants, like Pb and As, are almost totally (80-90%) bound to sediments 41, 23 and 24, presumably to muscovite and biotite mica. These speculations can be supported with literature results [42]. Only Mn in samples 23, 24 and 14R, which is easily soluble in aqua regia (92-100%) can be important for further biological and toxicological studies.

Grain size analysis

In a separate geomorphological study [43] cumulative curves of fluvial deposits were studied in the main flow of Kupa River. There is a general fining of grain size downstream. In the present work, only silt + clay fraction was studied, the same one on which elemental concentrations were determined. Because of low clay content, it can be suggested that silt fraction contains most of trace elements. The particle size measurements on the clay-to-sand-size sediment are an important source of information about their provenance, transport and depositional conditions. The surface-area determination can be used in combination with solution data, when available, to reach a conclusion about the trace-element adsorption capacity of the studied sediments. In the present work we used the laser-diffraction method to study the particle size and the geometric surface area, which is a relatively fast and simple method in comparison with classical methods. It should be noted, however, that there are various classic and more modern techniques in use, to determine the particle size [44-49]. Each technique defines the size of a particle in a different way, and thus measures different properties of the same material [50]. For a particle size determination of stream sediments any one of these methods would be satisfactory. For more detailed research on adsorption capacity of contaminated sediments, instead of geometric surface area, specific surface area can be determined by the BET technique [51].

Mössbauer spectroscopy

The Mössbauer spectroscopy was used to evaluate potential iron-containing sinks for heavy-metal adsorption, like Meaz et al. [52] in their investigation of sediments in the Great Nile. The determined sediment ratio of Fe^{3+}/Fe^{2+} is consistent with a predominantly ferric rather than ferrous phase in samples 14R and 23. Oxidative precipitation, influenced by Mn oxides, is a possible explanation, because in these two samples Mn extreme and Mn outlier were reported by Frančišković-Bilinski [13], out of a large data set from the Kupa River drainage basin. This finding supports the work of Van Der Zee et al. [53], who studied the iron redox transition of Fe^{2+} by Mn oxides in marine sediments. Iron redox reactions need to be studied because they have the potential to support a substantial microbial population in soil and sedimentary environments [54]. Iron hydrous oxides and oxides, identified at 70 K are important adsorbents for trace elements [55] and for natural organic matter [56]. Therefore identification of iron hydrous oxides and oxides obtained by Mössbauer spectroscopy can be indirectly related to sediment quality evaluation.

Solid-state NMR

The ^{29}Si MAS NMR and ^{27}Al MAS NMR techniques are rather complicated and are not practical for being adopted for a wide scale use during monitoring in all locations studied. However, their application and sedimentary research on selected samples can be useful in comparison with XRD results. One has to be aware that the presence of Fe and other paramagnetic impurities seriously reduces the quality of ^{29}Si NMR spectra in complex mixture of sediments. The weakest ^{29}Si NMR spectrum was obtained in sample 24, where Fe anomaly is present [13]. However, this method was very successfully applied when pure minerals [57] and synthetic samples [58] were studied. ^{27}Al MAS NMR is more promising in sediment studies. The finding of muscovite is significant, because of its adsorption properties for arsenite and arsenate [42]. In the chapter of elemental analysis of this paper was described that As was totally bound to sediments. Aluminum coordination changes, which can be studied by solid state NMR are known to be related to aluminosilicate dissolution [59], which can be possible secondary source of pollution with adsorbed trace elements.

CONCLUSIONS

The described complementary multi-instrumental methods were applied on selected stream sediments out of the large dataset to illustrate the advantages and disadvantages of particular methods in physico-chemical assessment (first part of TRIAD approach):

The mineralogical analysis, performed with the XRD powder method, detected major, minor and trace minerals, mostly from tectosilicate, phyllosilicate and carbonate class. The composition of clay minerals, present in <5%, is less certain and other complementary methods should be applied for amorphous and poorly crystalline phases.

The difference in concentrations of elements performed with XRF in total sample and ICP-MS in aqua regia extract can be used to identify trace elements firmly bound to the mineral structure. They should not be necessarily further studied by biological and toxicological studies (in this work Cr, As, Pb). Toxic elements loosely bound in this work (Mn) should be further studied, if the concentration is above the level causing significant toxicity, like in samples 23, 24 and 14R.

The grain-size analysis gives information about the amount of clay size particles in silt+clay fraction, which can be easily transported in downstream direction, carrying pollutants.

The Mössbauer spectroscopy gives information about Fe compounds, like hematite and goethite, which are known significant sinks for trace elements. Determination of ferric and ferrous phases is important for microbial population [54].

The NMR spectroscopy was applied to study aluminum and silicate minerals, both crystalline and amorphous. Important pollutant sinks like muscovite and kaolinite, suggested from XRD results, could be confirmed by NMR. Changes of aluminium coordinations could be related to possible alumino silicate dissolution, according to Criscenti et al. [59] and thus be of significance for secondary sources of pollutants. During this process pollutants incorporated in the structure or adsorbed on alumino silicates are released and secondary sources of pollutants can occur.

The application of the presented complementary multi-instrumental methods can be recommended in initial stage of stream sediment investigation. It gives information about mixture of crystalline, poorly crystalline and almost amorphous minerals, some of which are very good adsorbents for trace elements. Possible sinks and secondary sources can be identified. It can be suggested that after the physico-chemical assessment is decided if and in which region the other two steps in TRIAD monitoring are to be applied. It is aimed in the future that monitoring network and water management can be precisely established.

ACKNOWLEDGMENTS

This research was supported by the Ministry of Science, Education and Sport of the Republic of Croatia, project 0098041 (2002-2006; principal investigator H. Bilinski) and project 098-0982934-2720 (principal investigator I. Pižeta), by the bilateral project Croatia-Slovenia 2004-2005 (principal investigators H. Bilinski and D. Hanžel) and by the bilateral project Croatia-Hungary 2005-2007, project No. HR-14/2004 (principal investigators H. Bilinski and G. Szalontai). The authors thank D. Tibljaš (Croatia) and P. Kump (Slovenia) for allowing us to use their equipment and programs for XRD and XRF, respectively. Special thanks go to Professor Attila Vertes for his valuable comments regarding Mössbauer results. The paper has been edited by Dr. Paul McGuiness, a native English speaker and physicist at IJS, Ljubljana.

REFERENCES

[1] Ávila, P.F., Oliveira, J.M.S., Da Silva, E.F. and Fonseca, E.C. (2005). Geochemical signatures and mechanisms of trace elements dispersion in the area of the Vale das Gatas mine (Northern Portugal). *Journal of Geochemical Exploration* **85**, 17-29.

[2] Albanese, S., De Vivo, B., Lima, A. and Cicchella, D. (2007). Geochemical background and baseline values of toxic elements in stream sediments of Campania region, Italy. *Journal of Geochemical Exploration* **93**, 21-34.

[3] Hochella, M.F., Jr. (2002). Sustaining Earth: Thoughts on the present and future roles of mineralogy in environmental science. *Mineralogical Magazine* **66(5)**, 627-652.

[4] Valsami-Jones, E., Polya, D.A. and Hudson-Edwards, K. (2005). Environmental mineralogy, geochemistry and human health. *Mineralogical Magazine* **69(5)**, 615-620.

[5] Förstner, U. and Heise, S. (2006). Assessing and managing contaminated sediments: Requirements on data quality - from molecular to river basin scale. *Croatica Chemica Acta* **79**, 5-14.

[6] Babut, M.P., Ahlf, W., Batley, G.E., Camusso, M., De Deckere, E and Den Besten, P.J. (2003). International overview of sediment quality guidelines and their uses. In: Wenning, R.J., Ingersoll, C.G., Batley, G.E. (Eds.) Use of sediment quality guidelines and related tools for the assessment of contaminated sediments – SETAC. Online available at www.setac.org

[7] Quevauviller, P. (2007). European analytical quality control in support of the water framework directive via the water information system for Europe – EAQC WISE. European Commission DG Research funded project under the Sixth Framework Programme (contract n°022603), Newsletter-issue 1, March 2007.

[8] Den Besten, P.J., De Deckere, E., Babut, M., Power, R.B., Del Valls, T.A., Zago, C., Oen, A.M. and Heise, S. (2003). Biological effects-based sediment quality in ecological risk assessment for European waters. *Journal of soils and sediments* **3**, 144-162.

[9] Long, E.R. and Chapman, P.M. (1985). A sediment quality triad, measures of sediment contamination, toxicity and infaunal community composition in Pudget Sound. *Marine Pollution Bulletin* **16**, 405-415.

[10] Frančišković-Bilinski, S., Bilinski, H. and Širac, S. (2005). Organic pollutants in stream sediments of Kupa River drainage basin. *Fresenius Environmental Bulletin* **14**, 282-290.

[11] Frančišković-Bilinski, S. (2005). Geochemistry of stream sediments in Kupa River drainage basin, Dissertation. University of Zagreb, 197 pp.

[12] Frančišković-Bilinski, S. (2006). Barium anomaly in Kupa River drainage basin. *Journal of Geochemical Exploration* **88(1-3)**, 106-109.

[13] Frančišković-Bilinski, S. (2007). An assessment of multielemental composition in stream sediments of Kupa River drainage basin, Croatia for evaluating sediment quality guidelines. *Fresenius Environmental Bulletin* **16(5)**, 561-575.

[14] Frančišković-Bilinski, S. (2008). Detection of coal combustion products in stream sediments by chemical analysis and magnetic susceptibility measurements. *Mineralogical Magazine* **72(1)**, 43-48.

[15] Bilinski, H. (2008). Weathering of sandstones studied from the composition of stream sediments of the Kupa River (Croatia). *Mineralogical Magazine* **72(1)**, 23-26.

[16] SMSP and FALCONBRIDGE NC SAS (2005). Koniambo project, Environmental and social impact assessment, Chapter 4 Mine, 4.2-7 Quality criteria for freshwater sediment.

[17] Frančišković-Bilinski, S., Bilinski, H., Grbac, R., Žunić, J., Nečemer, M. and Hanžel, D. (2007). Multidisciplinary work on barium contamination of the karstic upper Kupa River drainage basin (Croatia and Slovenia); calling for watershed management. *Environmental Geochemistry and Health* **29(1)**, 69-79.

[18] Dragun, Z., Raspor, B. and Podrug, M. (2007). The influence of the season and the biotic factors on the cytosolic metal concentrations in the gills of the European chub (*Leuciscus cephalus L.*). *Chemosphere* **69(6)**, 911-919.

[19] Källqvist, T., Milačič, R., Smital, T., Thomas, V.K., Vranes, S., Tollefsen, K.-E. (2008). Chronic toxicity of the Sava River (SE Europe) sediments and river water to the algae *Pseudokirchneriella subcapitata*. *Water Research* **42**, 2146-2156.

[20] Bilinski, H., Frančišković-Bilinski, S., Nečemer, M., Hanžel, D., Szalontai, G. and Kovacs, K. (2007). Complementary methods for characterization of stream sediments as an aid in assessment of sediment quality. Goldschmidt Conference Abstracts, *Geochimica Cosmochimica Acta* **71**, supplement 1, A92.

[21] Brils, J. (2008). Sediment monitoring and the European Water Framework Directive. *Ann. Inst. Super Sanità* **44(3)**, 218-223.

[22] Tukey, J.W. (1977). Exploratory data analysis. Addison-Wesley, Reading, Mass.

[23] Powder Diffraction File (1997). International Center for Diffraction Data, Newtown Square, PA, USA.

[24] Boldrin, A., Juračić, M., Mengazzo Vitturi, L., Rabitti, S. and Rampazzo, G. (1992). Sedimentation of river-borne material in a shallow shelf sea: Adiga River, Adriatic Sea. *Marine Geology* **103**, 473-485.

[25] Salminen, R. and Tarvainen, T. (1997). The problem defining geochemical baselines. A case study of selected elements and geological materials in Finland. *Journal of Geochemical Exploration* **60**, 91-98.

[26] Kump, P., Nečemer, M., Smodiš, B. and Jaćimović, R. (1996). Multielement analysis of rubber samples by X-ray fluorescence. *Applied Spectroscopy* **50**, 1373–1377.

[27] Van Espen, P. J. M. and Janssens, K. H. A. (1993). Spectrum evaluation. In Van Grieken R. E. & Markowicz A. A. (Eds.), Hand book of X-ray spectroscopy; methods and techniques. New York: Marcel Dekker.

[28] National Bureau of Standards (1988). Certificate of analysis: Standard Reference Material 2704, Buffalo River Sediment. Gaithersburg, MD, USA.

[29] Salomon, S., Jenne, V., and Hoenig, M. (2002). Practical aspects of routine trace element environmental analysis by inductively coupled plasma – mass spectrometry. *Talanta* **57**, 157-168.

[30] Wentworth, C.K. (1922). A scale of grade and class terms for clastic sediments. *Journal of Geology* **30**, 377-392.

[31] Pollak, H. and Stevens, J.G. (1988). Phyllosilicates: A Mössbauer evaluation. *Hyperfine Interactions* **29**, 1153-1156.

[32] Bilinski, H., Giovanoli, R., Usui, A. and Hanžel, D. (2002). Characterization of Mn oxides in cemented streambed crusts from Pinal Creek, Arizona, U.S.A., and in hot-spring deposits from Yuno-Taki Falls, Hokkaido, Japan. *American Mineralogist* **87**, 580-591.

[33] Engelhardt, G. and Michel, D. (1991). High-Resolution Solid-State NMR of silicates and zeolites. John Wiley & Sons, New York.

[34] Akitt, J.W. (1989). Multinuclear studies of aluminium compounds. *Progress in NMR Spectroscopy* **21**, 1-149.

[35] Ashbrook, S.E., McManus, J., MacKenzie, K.J.D. and Wimperis, S. (2000). Multiple-Quantum and cross-polarized ^{27}Al MAS NMR of mechanically treated mixtures of kaolinite and gibbsite. *Journal of Physical Chemistry B*, **104**, 6408-6416.

[36] Duar, M.J. (2004). Introduction to Solid-state NMR spectroscopy. Blackwell Publishing, Oxford.

[37] Lee, S.K., Stebbins, J.F., Weiss, C.A. and Kirkpatrick, R.J. (2003). O-17 and Al-27 MAS and 3QMAS NMR study of synthetic and natural layer silicates. *Chemistry of Materials* **15(13)**, 2605-2613.

[38] Wang, Alian and Valentine, R.B. (2002). Seeking and identifying plyllosilicates on Mars – A simulation study. *Lunar and Planetary Science* **33**, 1370.

[39] Frančišković-Bilinski, S., Bilinski, H., Tibljaš, D. and Hanžel, D. (2003). Estuarine sediments from boreal region – an indication of weathering. *Croatica Chemica Acta* **76(2)**, 167-176.

[40] Brown Jr., G.E. and Parks, G.A. (2001). Sorption of trace elements from aqueous media: Modern perspectives from spectroscopic studies and comments on adsorption in the marine environment. *International Geological Reviews* **43**, 963-1073.

[41] Skoog, D.A., Holler, F.J., Nieman, T.A. (1998). Principles of instrumental analysis, 5th Edition. Harcourt Brace College Publishers, Florida, 288 p.

[42] Chakraborty, S., Wolthers, M., Chatterjee, D. and Charlet, L. (2007). Adsorption of arsenite and arsenate onto muscovite and biotite mica. *Journal of Colloid and Interface Science* **309**, 392-401.

[43] Frančišković-Bilinski, S., Bhattacharya A.K. (2009). Channel processes and sedimentation in the Kupa River (Croatia). *Goldschmidt Conference Abstracts 2009, supplement to Geochimica et Cosmochimica Acta* (Podosek, Frank A. Ed.), Davos, Switzerland, A392-A392.

[44] McCave, I.N., Bryant, R.J., Cook, H.F., Coughanowr, C.A. (1986). Evaluation of a laser-diffraction-size analyzer for use with natural sediments. *Journal of Sedimentary Petrology* **56**, 561-564.

[45] Singer, J.K., Anderson, J.B., Ledbetter, M.T., McCave, I.N., Jones, K.P.N., Wright, R. (1988). An assessment of analytical techniques for the size analyisis of fine-grained sediments. *Journal of Sedimentary Petrology* **58**, 534-543.

[46] Balagurunathan, Y., Dougherty, E.R., Frančišković-Bilinski, S., Bilinski, H. and Vdović, N. (2001). Morphological granulometric analysis of sediment images. *Image Analysis and Stereology* **20(2)**, 87-99.

[47] Frančišković-Bilinski, S., Bilinski, H., Vdović, N., Balagurunathan, Y. and Dougherty, E.R. (2003). Application of image-based granulometry to siliceous and calcareous estuarine and marine sediments. *Estuarine Coastal and Shelf Science* **58(2)**, 227-239.

[48] Graham, D.J., Rice, S.P. and Reid, I. (2005). A transferable method for the automated grain sizing of river gravels. *Water Resources Research* **41**, 1-12.

[49] Iatrou, M., Papatheodorou, G., Piper, D.J.W., Tripsanas, E. and Ferentinos, G. (2007). A debate on the similarity of particle sizing results derived from the analysis of fine-grained sediments by two different instrumentations. *Bulletin of the Geological Society of Greece* **37**, Proceedings of the 11th International Congress, Athens, May 2007.

[50] Konert, M. and Vandenberghe, J. (1997). Comparison of laser grain-size analysis with pipette and sieve analysis: a solution for the underestimation of the clay fraction. *Sedimentology* **44**, 523-535.

[51] Brunauer, S., Emmett, P.H. and Teller, E. (1938). Adsorption of gases in multimolecular layers. *Journal of the American Chemical Society* **60**, 309-319.

[52] Meaz, T.M., Amer, M.A. and Koch, C.B. (2004). Iron-containing adsorbents in Great Nile sediments. *Hyperfine Interactions* **156(1)**, 465-469.

[53] Van Der Zee, C., Slomp, C.P., Rancourt, D.G., De Lange, G.J. and Van Raaphorst, W. (2005). A Mössbauer spectroscopic study of the iron redox transition in eastern Mediterranean sediments. *Geochimica et Cosmochimica Acta* **69(2)**, 441-453.

[54] Weber, K.A., Achenbach, L.A. and Coates, J.D. (2006). Microorganisms pumping iron: anaerobic microbial iron oxidation and reduction (Review). *Nature Reviews. Microbiology* **4(10)**, 752-764.

[55] Peacock, C.L. and Sherman, D.M. (2004). Copper (II) sorption onto goethite, hematite and lepidocrocite: a surface complexation model based on ab initio molecular geometries and EXAFS spectroscopy. *Geochimica et Cosmochimica Acta* **68**, 2623-2637.

[56] Genz, A., Baumgarten, B., Goernitz, M. and Jekel, M. (2008). NOM removal by adsorption onto granular ferric hydroxide: Equilibrium, kinetics, filter and regeneration studies. *Water Research* **42**, 238-248.

[57] Welch, M.D., Liu, S.X. and Klinowski, J. (1998). Si-29 MAS NMR systematics of calcic and sodic-calcic amphiboles. *American Mineralogist* **83**, 85-96.

[58] Welch, M.D., Pawley, A.R., Ashbrook, S.E., Mason, H.E. and Phillips, B.L. (2006). Si vacancies in the 10-Å phase. *American Mineralogist* **91**, 1707-1710.

[59] Criscenti, L.J., Brantley, S.L., Mueller, K.T., Tsomaia, N. and Kubicki, J.D. (2005). Theoretical and 27Al CPMAS NMR investigation of aluminum coordination changes during aluminosilicate dissolution. *Geochimica et Cosmochimica Acta* **69**, 2205-2220.

Received: October 19, 2009
Revised: November 11, 2009
Accepted: November 17, 2009

CORRESPONDING AUTHOR

Stanislav Frančišković-Bilinski
Institute "Ruđer Bošković"
POB 180
10002 Zagreb
CROATIA

E-mail: francis@irb.hr